T. RZYCHOŃ*, A. KIEŁBUS*

MICROSTRUCTURE AND TENSILE PROPERTIES OF SAND CAST AND DIE CAST AE44 MAGNESIUM ALLOY

MIKROSTRUKTURA I WŁAŚCIWOŚCI MECHANICZNE ODLEWANEGO DO FORMY PIASKOWEJ I CIŚNIENIOWO STOPU MAGNEZU AE44

The AE44 magnesium alloy was prepared by gravity and die casting methods. The microstructure and mechanical properties were investigated. The results demonstrated that microstructure of sand casting consist of large grains of α solid solution and needle-shaped $Al_{11}RE_3$ phase, globular particles of $Al_{10}RE_2Mn_7$ and small volume fraction of Al_2RE. Die casting process caused significant refinement of structure and change of phase composition. Die cast AE44 alloy consists of $Al_{11}RE_3$ phase and precipitates of Al_2RE and $Al_{2.12}RE_{0.88}$ compounds. The mechanical properties at room and elevated temperature of the sand cast alloy are relatively low due to coarse-grain structure. Die-casting process increases the ultimate tensile strength, yield strength and elongation of AE44 magnesium alloy.
Keywords: Mg-Al-RE alloys, microstructure, mechanical properties

W pracy przedstawiono wyniki badań mikrostruktury i właściwości mechanicznych stopu magnezu AE44 po odlewaniu do formy piaskowej i ciśnieniowym. Mikrostrukturę odlewu piaskowego charakteryzuje znaczna gruboziarnistość i obecność faz międzymetalicznych $Al_{11}RE_3$, $Al_{10}RE_2Mn_7$ i Al_2RE, której udział objętościowy jest nieznaczny. Zastosowanie odlewania ciśnieniowego powoduje silne rozdrobnienie mikrostruktury i zmiany składu fazowego. W odlewie ciśnieniowym obserwuje się iglastą fazę $Al_{11}RE_3$ oraz wydzielenia faz Al_2RE i $Al_{2.12}RE_{0.88}$. Właściwości mechaniczne odlewu piaskowego w temperaturze otoczenia i podwyższonej są stosunkowo niskie. Po odlewaniu ciśnieniowym obserwuje się podwyższenie wytrzymałości na rozciąganie, granicy plastyczności oraz wydłużenia.

1. Introduction

Magnesium alloys represent the lightest class of metal alloys for structural applications. They offer a good combination of castability, mechanical strength and ductility [1]. Magnesium alloys are usually produced by high-pressure die casting providing high productivity at a relatively low cost [2]. The fluidity of magnesium in the molten state allows for easy manufacturing of thin-walled components. The use of these components in the automotive industry is an increasing trend and includes steering wheels, engine components, seat frames and instrument panels [3]. More effective weight reductions could be achieved by applying magnesium alloys to powertrain parts operate at elevated temperature, e.g. above 180°C. The most common magnesium alloy for die casting is AZ91 (Mg-9Al-0.8Zn), which offers a good combination of mechanical properties at room temperature. However the AZ91 alloy is unsuitable for applications at temperatures above 120°C due to reduced creep resistance. The poor elevated temperature properties of Mg-Al based alloys are related to presence of low-melting $Mg_{17}Al_{12}$ phase. The improvement of creep resistance of Mg-Al alloys can obtain by addition of alloying elements such as silicon, strontium, calcium or rare earth elements. The promising alloys for lightweight applications in the automotive industry are AE series alloys (Mg-Al-RE) [4-7]. Typical representative of this system is AE42 (Mg-4Al-2RE) die casting alloy, which exhibits good creep resistance, due to the presence of high-melting $Al_{11}RE_3$ phase and absence of $Mg_{17}Al_{12}$ compound [8,9]. However, the problem of instability may appear above 150 °C. According to Powell et al. [9], the $Al_{11}RE_3$ phase is unstable during long-term creep and annealing at elevated temperature and decomposes to the Al_2RE compound, releasing some Al atoms that subsequently react with Mg atoms to form the unwanted

* DEPARTMENT OF MATERIAL SCIENCE, SILESIAN UNIVERSITY OF TECHNOLOGY, KATOWICE, POLAND

$Mg_{17}Al_{12}$ phase. Finally, the above process leads to the deterioration of creep resistance of AE42 alloy. Recently, Hydro Magnesium has developed a new die-casting alloy, AE44 (Mg-4Al-4RE). It was shown that this alloy has better creep resistance at 175 °C than AE42 alloy. However the relationship between microstructure and higher creep resistance is still unclear [10,11]. In this paper we investigated the microstructure of a sand cast and die-cast AE44 alloy and their mechanical properties at room and elevated temperatures.

2. Experimental

The investigations were performed on the AE44 (Mg-4.15wt.%Al-4.01wt.%RE-0.36wt.%Mn) sand-cast and die-cast alloy. The rare earth additions (RE) were made as mischmetal with the approximate compositions: 50 wt% cerium, 26 wt% lanthanum, 15 wt% neodymium and 3 wt% praseodymium.

Melting of the AE44 alloy was conducted in a mild steel crucible under the protection of a self-made flux. The melt was held at 750 °C for several minutes then poured into sand mould at 735 °C. Die cast samples of AE44 magnesium alloy were obtained using hot chamber die casting machine. The melt was protected by a mixed gas atmosphere of SF_6 and CO_2. The melt and die temperatures for investigated alloy were 680 °C and 150 °C, respectively. The plunger velocity in the second phase was 350 cm/s.

The microstructure was characterized by optical microscopy (Olympus GX-70), a scanning electron microscopy (Hitachi S4200) equipped with a energy dispersive spectrometer (THERMO NORAN). A quantitative metallography was made by a surface method, using the Met-Ilo computer program [12].

X-ray diffraction patterns were collected using X-Pert Philips diffractometer equipped with curved graphite monochromator on diffracted beam and with the following slits (in the sequence form Cu tube counter); Soller (2°), divergence (1/2°), antiscatter (1/2°) and receiving (0.15 mm). The X-ray data collection was performed for 10-140° 2θ range with 0.02° step.

Tensile testing of the as-cast bars at ambient and elevated (150 °C) temperature was performed in a MTS-810 material test machine.

3. Results and discussion

3.1. Microstructure

The cast structures observed for sand cast alloy and die cast alloy are presented in Fig. 1.The typical cast structure consisting of three zones (chill, columnar and equiaxed zone) is observed for sand cast AE44 alloy (Fig. 1a). The mean grain size in the equiaxed zone is equal ≈1 mm. Die cast AE44 alloy only shows a fine equiaxed grain structure (Fig. 1a). High pressure die casting results in a decrease in the grain size (the mean grain size is 8,2 μm). The average grain size increases with the increasing distance from the sample edge as is illustrated by Fig. 1b and 1c.

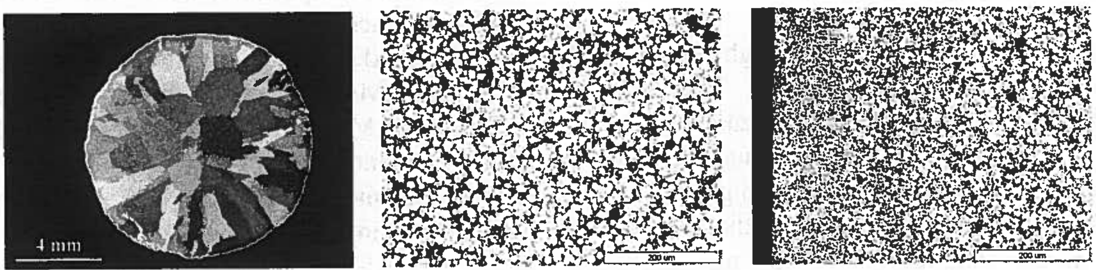

a) b) c)

Fig. 1. Grain structures of AE44 magnesium alloy; sand cast (a); at the centre of die cast (b); at the surface of die cast (c)

The grain size of sand cast AE44 alloy was much larger than that of diecast AE44. This can be attributed to the difference in solidification rates. In die casting, molten metal is forced into a steel mold by high pressure and velocity, and is held under pressure during solidification so that the molten metal fills the mold completely and rapidly. Therefore the solidification occurs very rapidly in pressure die casting and is much faster than in the slowly cooled sand castings.

Fig. 2 shows unetched microstructure of the diecast specimen. Shrinkage and gas porosity is observed in microstructure. The gas porosity is mainly due to the trapped air in the die cavity during die-cast process and dissolved gases in the liquid alloy, whereas the shrinkage porosity is due to thermal contraction of metal during solidification. Distribution of shape factor of pores (defined as d_{max}/d_{min}, d – diameter of pore) indicates that gas pores are dominant in microstructure.

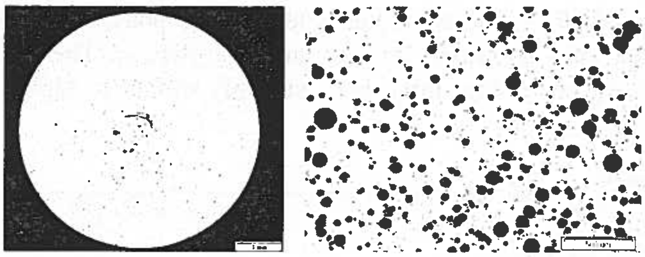

a)

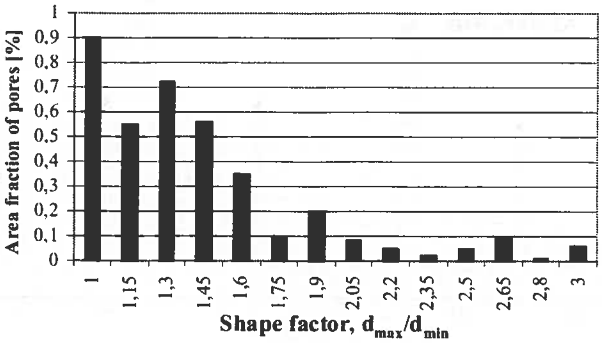

b)

Fig. 2. The porosity in AE44 magnesium alloy (a); distribution of shape factor of pores (b)

Pt	Chemical composition at.-%						Al/RE
	Mg	Al	Mn	La	Ce	Nd	
A	8,4	73,4		6,2	11,1	0,9	4,0
B	6,85	63,9		5,9	19,2	4,2	2,2
C	5.6	55.2	35.0		4.2		
D	99.4	0,6					

a)

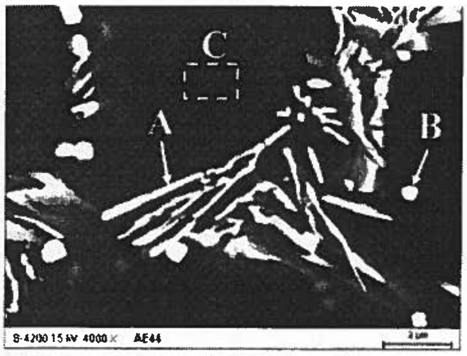

Pt	Chemical composition at.-%					Al/RE
	Mg	Al	La	Ce	Nd	
A	80.3	15.7	1.1	2.9	-	3,9
B	82.7	12.4	1.8	2.8	0.3	2,5
C	97.9	1.3				

b)

Fig. 3. The SEM image and EDS results of (a) sand cast and (b) die cast alloys

Typical microstructure of gravity-cast is shown in Fig. 3a. The main constituents of sand cast, besides α-Mg, are the needle-shaped RE-rich precipitates and globular or irregular particles containing manganese and rare earth elements.

Fig. 3b shows the microstructure of die-cast specimen. AE44 magnesium alloy consists of primary α-Mg grains with the acicular and globular phases at the grain boundaries. The microanalysis performed on these phases with EDS system indicated that acicular precipitates contain aluminum and rare earth elements. The ratio of Al/RE is about 4. In the globular compounds the ratio Al/RE is close to 2.

In order to identify the existing phases in the alloy, XRD analysis was performed (Fig. 4). Results of XRD analysis show the main intermetallic phase in sand-cast AE44 alloy is $Al_{11}La_3$. Basing on the XRD pattern and results of microanalysis of acicular particles in this alloy, they can be ascribed as $Al_{11}La_3$, with some cerium substituting lanthanum. The molecular formula of these phases is represented by $Al_{11}RE_3$. Moreover the Al_2RE and $Al_{10}RE_2Mn_7$ phases were identified in the alloy. In die-cast alloy (Fig. 5), except α-Mg, three intermetallic phases were identified e.g. $Al_{11}RE_3$, Al_2RE and $A_{l2.12}RE_{0.88}$. The peak positions for $A_{l2.12}RE_{0.88}$ are strongly shifted to higher angles.

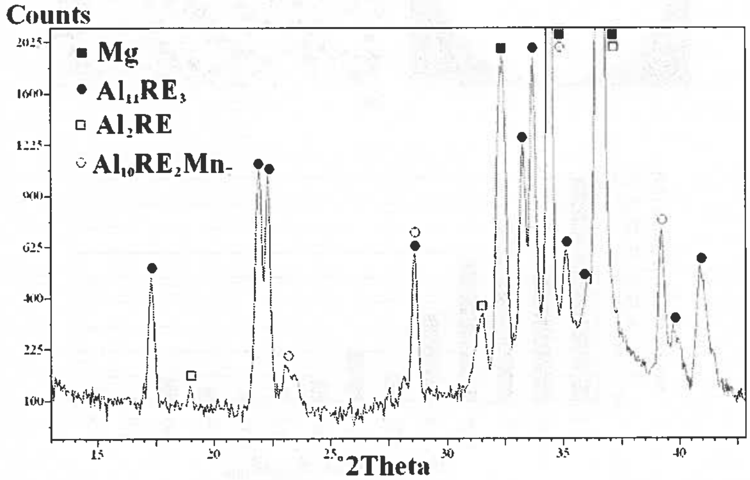

Fig. 4. XRD pattern of sand cast AE44 alloy

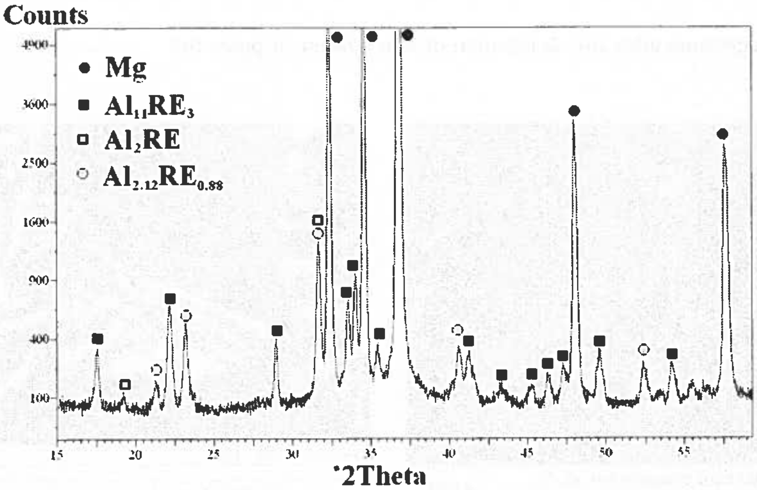

Fig. 5. XRD pattern of die cast AE44 alloy

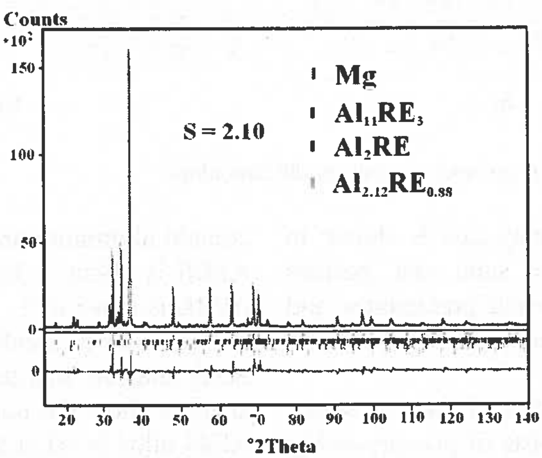

Fig. 6. X-ray diffraction pattern fitting by Rietveld refinement of die cast AE44 alloy

The results of XRD analysis indicate that AE44 is multiphase alloy. Therefore, in order to verify obtained results the Rietveld method was used [14]. Because of the low intensity of the diffraction lines for secondary phases, the positional coordinates and isotropic thermal parameters were fixed to the proper values. Only scale factor, lattice parameters, FWHM (full width at half maximum) parameters, background parameters, profile asymmetry and specimen displacement were refined for this alloy. The phase abundance by weight was calculated by using the relation proposed by Hill and Howard [15]. The Rietveld refinement plot of the die-cast specimen is presented in Fig. 6 and the information on the phase concentration is presented in Table 2. The fitting of calculated pattern to the experimental one seems to be sufficient (S = 2.10). The $Al_{11}RE_3$ phase is dominant compound in the structure of die-cast, whereas the content of Al_2RE compound is neglible. These compounds are typical in Mg-Al-RE alloys [9,10]. The $Al_{2.12}RE_{0.88}$ was prepared by annealing at 1200 °C and water quenching [18]. We assume that the presence of $Al_{2.12}RE_{0.88}$ phase in AE44 alloy is due to rapid crystallization of AE44 die-cast alloy and macrosegregation of alloying elements, especially of rare earth elements. The $Al_{2.12}RE_{0.88}$ phase has smaller lattice parameters than those the values tabulated in ICDD card. It is consistent with some cerium and neodymium substituting lanthanum in the crystal lattice.

TABLE 1

Phase contents and their lattice parameters for die-cast alloy

Phase	Space group	Contents [wt.%]	Lattice parameters [nm]	
			Rietveld	ICDD
Mg	$P6_3/mmc$	95,0(3)	a_0= 0.32056(6) c_0= 0.5206(1)	a = 0.3209 c = 0.5211
$Al_{11}RE_3$	Immm	3,52(4)	a_0= 0.43772(9) b_0=1.0124(2) c_0=1.3050(3)	a = 0.4431 b = 1.013 c = 1.3142
Al_2RE	Fd-3m	0,12(8)	a_0= 0.8025(2)	a = 0.8052
$Al_{2.12}RE_{0.88}$	P6/mmm	1,37(4)	a_0= 0.44341(9) c_0= 0.41732(8)	a= 0.4478 c= 0.4347

In investigated alloy only Al-RE or Al-RE-Mn were detected. According to Wei and Dunlop [17], because of the high chemical stability of $Al_{11}RE_3$, rare earth elements are combined with aluminum and form these phases until all the available RE were used without any formation of pseudobinary Mg-RE or pseudoternary Mg-Al-RE phases.

3.2. Mechanical properties

The tensile test data obtained for both sand-cast and die-cast alloys at room and 175 °C temperature are given in Table 2. The sand-cast alloy has low tensile strength and elongation both at room and elevated temperature, which should be attributed to its coarse-grain microstructure.

TABLE 2

Mechanical properties of sand and die cast alloy at room and elevated temperature

State	Room Temperature			175 °C		
	UTS, MPa	YS, MPa	El., %	UTS, MPa	YS, MPa	El., %
Sand-cast	146.0±1.4	47±2.2	7.1±0.4	98.5±5.1	42.8±1.1	10.6±0.4
Die-cast*	240±8	178±10	11.8±3.2	129±3	114±1	28.2±4.1

* The results were obtained for samples with porosity below 1.5 %.

The SEM micrographs of the gravity-cast alloys tested at room temperature are shown in Fig. 7. In Fig. 7a, ductile dimples, cleavage facets and cracks can be clearly observed. The presence of cleavage facets is related to the hexagonal close-packed crystal structure of magnesium and restriction of slip systems. In Fig. 7b, it can be seen that the $Al_{11}RE_3$ needle-shaped are particles irregularly distributed in the matrix. The cracks mainly initiate at the $Mg/Al_{11}RE_3$ interface or inside of the $Al_{11}RE_3$ phase. The growth and coalescence of the microcracks eventually caused the failure of the specimen.

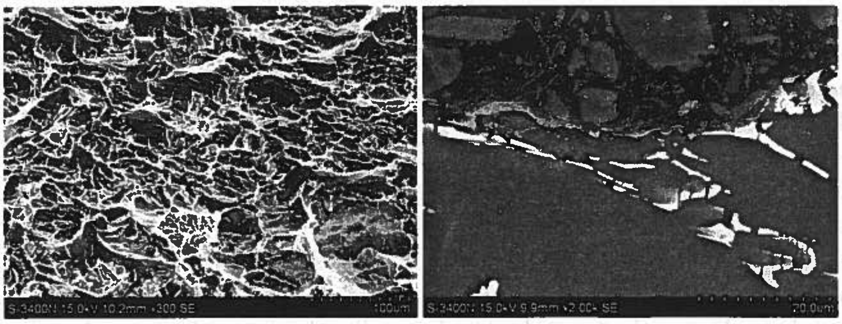

Fig. 7. SEM fractograph of the (a) surface, (b) vertical section of the specimen failed in the tensile test of sand cast AE44 magnesium alloy

The die-casting process caused a considerable increase in tensile strength and elongation compared to sand-cast alloy. However its mechanical properties are very sensitive on the volume fraction of gas pores in the microstructure (Fig. 8). Only the samples with porosity below 1.5 % present satisfactory mechanical properties, i.e. UTS ≈ 240 MPa and YS ≈ 180 MPa.

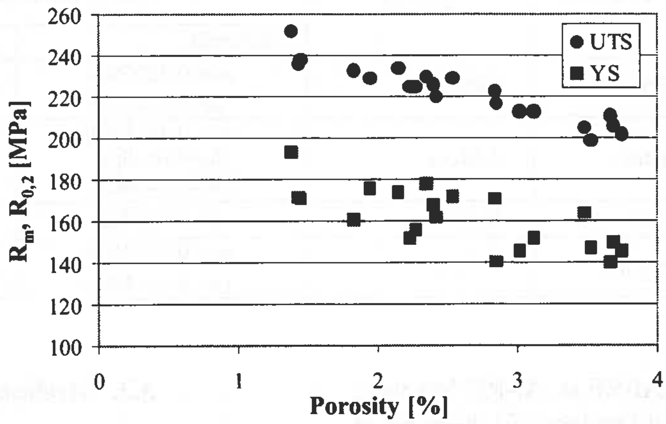

Fig. 8. The influence of porosity on tensile and field strength of die cast AE44 alloy

The increase of mechanical properties of die-cast alloy is due to fine-grain microstructure with intermetallic network at the grain boundaries, as well as to the solid solution strengthening of the matrix by aluminum. Fig. 9 shows typical SEM view of ductile fracture the die-cast alloy with elongated shrinkage porosity and spherical gas (air) porosity.

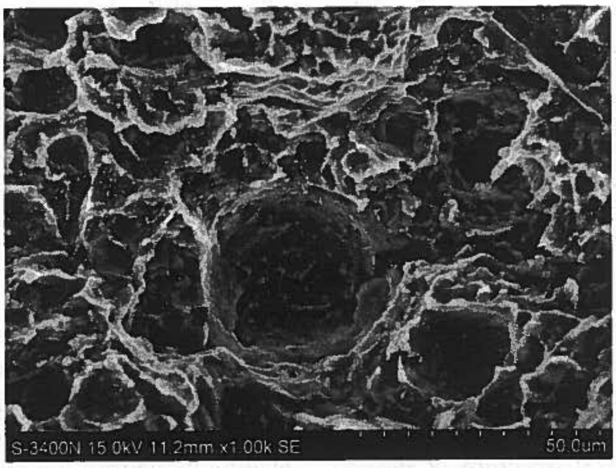

Fig. 9. Tensile fracture of die-cast AE44 magnesium alloy tested at room temperature

4. Conclusion

The microstructure and mechanical properties of sand and die cast AE44 magnesium alloy have been investigated. The following conclusions can be drawn:

1. The microstructure of sand-cast AE44 magnesium alloy consists of α-Mg, needle-shaped $Al_{11}RE_3$, globular and irregular $Al_{10}RE_2Mn_7$ and regular Al_2RE phases. The mean grain size is $\approx$ 1 mm.
2. The fine grain microstructure of die cast AE44 magnesium alloy consists of α-Mg, nedlee shaped $Al_{11}RE_3$, globular $Al_{2.12}RE_{0.88}$ and Al_2RE phases. The mean grain size in alloy is 8,2 μm.
3. Die casting process applied to AE44 magnesium alloy improved mechanical properties at room and elevated temperatures. The tensile strength of die cast alloy may reach 240 MPa as long as porosity is kept below 1,5 %.

Acknowledgements

The present work was supported by the Polish Ministry of Science and Higher Education through project No PBZ-KBN-114/T08/2004.

REFERENCES

[1] H. Friedrich, B. Mordike (Eds), Magnesium Technology: Metallurgy, Design Data, Automotive Applications, Springer Verlag, 2006.

[2] E. Aghion, B. Bronfin, F. Von Buch, S. Schumann, H. Friedrich, Newly Developed Magnesium Alloys for Powertrain Applications, Journal of Metals, Novemeber 30-33 (2003).

[3] J. P. Weiler, J. T. Wood, R. J. Klassen, R. Berkmortel, G. Wang, Variability of skin thickness in an AM60B magnesium alloy die-casting, Materials Science and Engineering **A419**, 297-305 (2006).

[4] A. A. Luo, Recent Magnesium Alloy Development for Automotive. Powertrain Applications, Materials Science. Forum **419-4**, 57-65 (2003).

[5] M. O. Pekguleryuz, Development of Creep Resistant Magnesium Diecasting Alloys, Materials Science Forum **350-351**, 131-140 (2000).

[6] S. G. Lee, A. M. Gokhale, Visualization of three-dimensional pore morphologies in a high-pressure die-cast Mg-Al-RE alloy, Scripta Materialia **56**, 501-504 2007.

[7] Y. Wang, S. Guan, X. Zeng, W. Ding, Effects of RE on the microstructure and mechanical proerties of Mg-8Zn-4Al, Materials Science and Engineering **A416**, 109-118 (2006).

[8] K. Wei, L. -Y. Wei, R. Warren, Creep Behaviour and Microstructure of Magnesium Die Cast Alloys AZ91 and AE42, Materials Science Forum **546-549**, 73-76 2007.

[9] B. Powell, V. Rezhets, M. Balogh, R. Waldo, Microstructure and Creep Behavior in AE42 Magnesium Die-Casting Alloy, Journal of Metals, August **34-38** (2002).

[10] P. Bakke, H. Westengen, The role of rare earth elements in structure and property control of magnesium die casting alloys, Magnesium Technology 2005, Ed. by N.R. Neelameggham, H.I. Kaplan, B.R. Powell, TMS, **291-296** 2005.

[11] Hydro Magnesium, AE alloys – the new family of creep reistant die casting alloys, Diecaster Bulletin, No. 11, October 2004.

[12] J. Szala, Application of computer-aided image analysis methods for a quantitative evaluation of material structure (in Polish). Gliwice, Poland: Silesian University of Technology, 2001.

[13] R. A. Young, A. Sakhivel, T. S. Moss, C. O. Paiva-Santos, DBWS-9411 – an upgrade of the DBWS programs for Rietveld Refinement with PC and mainframe computers, Journal Applied Crystallography, **28**, 366-367 (1995).

[14] R. W. Young (Ed), The Rietveld method, IUCr Monograph on Crystallography, Vol. 5, Oxford Science Pub., 1993.

[15] R. J. Hill, C. J. Howard, Quantitative phase-analysis from neutron powder diffraction data using the Rietveld method Journal Applied Crystallography, **28**, 467 (1987).

[16] J. Gröbner, D. Kevorkov, R. Schmid-Fetzer, Thermodynamic modeling of Al-Ce-Mg phase equilibria coupled with key experiments, Intermetallics **10**, 415-422 (2002).

[17] L. Y. Wei, G. L. Dunlop, H. Westengen, Materials Science and Technology, **12**, 741-750 (1996).

[18] K. H. J. Buschow, The lanthanum-aluminium system, Philips Research Reports, **20**, 337-348 (1965).

Received: 20 June 2008.